

A numerical modeling approach to evaluate energy-efficient mechanical ventilation strategies

Bilal Yassine, Kamel Ghali*, Nesreen Ghaddar, Issam Srour, Ghassan Chehab

Faculty of Engineering and Architecture, American University of Beirut, P.O. Box 11-0236, Beirut 1107-2020, Lebanon

ARTICLE INFO

Article history:

Received 30 June 2012

Received in revised form 9 August 2012

Accepted 28 August 2012

Keywords:

Building materials
Mechanical ventilation
Energy efficiency

ABSTRACT

This paper investigates design features that can potentially reduce the energy consumed in attaining appropriate thermal comfort levels in typical residential buildings. A numerical model coupled with a PID controller is developed to predict the indoor air temperature that is adjusted via mechanical ventilation. The model is used to simulate and evaluate various scenarios of building wall layouts and materials. From the various simulation runs, the wall configurations and materials were refined to combinations that rendered the mechanical ventilation a feasible option for attainment of comfort for the largest number of hours per year. The runs were conducted for a typical residential apartment located in the city of Beirut, Lebanon, which is characterized by mild coastal climatic conditions. Different wall configurations were assumed for each of the living zone and the bedroom zone of the apartment. The simulation results suggest an optimal wall configuration comprised of a 5 cm layer of insulating strawboard sandwiched between a 2 cm × 10 cm wall made of masonry units consisting of Hempcrete (mixture of Portland cement, aggregates, and industrial hemp fibers) for the living zone, whereas the wall for the bedroom zone consists of a 10 cm of Hempcrete.

© 2012 Elsevier B.V. All rights reserved.

1. Introduction

Worldwide, the building sector accounts for 50% of total energy consumption [1]. This percentage is expected to increase with population growth and climate change compounding the problem of dwindling energy resources. In an effort to minimize this increase in the building's energy demand, there is a growing movement toward the design, construction, and operation of energy efficient buildings [2–4].

The majority of the research effort in this field [5–13] has focused on methodologies, innovations, and initiatives aimed at reducing the operational energy consumption. Examples include development of energy efficient electro-mechanical systems (e.g. HVAC units, lighting), use of renewable energy, and adoption of incentives for use of building envelopes that provide high insulation and air tightness.

One means of mitigating the increase in energy consumption is by relying on mechanical ventilation systems for cooling purposes and on the applications of natural (as compared to processed and manufactured) and recycled materials in building construction. Incorporation of natural ventilation systems and ceiling fans lead to a decrease in the usage of mechanical air conditioning systems

and help attain indoor air quality and thermal comfort at higher air temperatures.

Several studies have shown that mechanical ventilation contributes to energy efficient buildings especially for buildings with appropriate thermal mass and sufficient daily temperature swing from day to night. On the other hand, the use of natural material such as industrial hemp fibers mixed with concrete has been reported to have low heat conductivity in comparison with other building materials in construction; thus, it reduces the summer heat gains and winter heat losses [5].

Several studies have investigated the impact of ventilation on the internal indoor air temperature [6–9]. The key parameters related to the efficiency of ventilation can be divided into three categories: climatic factors, building material and control strategy parameters. An example of climatic factors is the outdoor air temperature, which includes mean daily temperature and diurnal temperature range, i.e. the climatic potential index. Building parameters include the building type, envelope openings such as windows and doors, building material and building structure. The flow rate and time period are determined by the control strategy when mechanical ventilation is applied (night ventilation, day time ventilation, full-day ventilation and no ventilation).

Kolokotroni and Aronis [6], Blondeau et al. [7], Breesch [8], Carriho da Graca et al. [9] and Eicker [10] concluded that the use of night ventilation contributes to energy efficient buildings especially for buildings with appropriate thermal mass and sufficient

* Corresponding author. Tel.: +961 1 350000x3438; fax: +961 1 744462.
E-mail address: ka04@aub.edu.lb (K. Ghali).

Nomenclature

A	area of the wall (m^2)
C_p	specific heat (J/kg K)
COP	coefficient of performance
G	rate of moisture generation inside the space
h	heat convection coefficient ($\text{W/m}^2 \text{K}$)
I	total solar radiation
K	thermal conductivity (W/m K)
K_c	proportional gain parameters
\dot{m}	mass flow rate
PID	proportional–integral–derivative controller
T	temperature in (K)
TI	integrative gain parameter
TD	derivative gain parameter
T	time (s)
q_{int}	internal heat load
V	volume of the space (m^3)
W	humidity ratio ($\text{kg H}_2\text{O/kg dry air}$)
X	axial direction

Greek letters

ρ	density
α	wall surface absorptivity

Subscripts

a	air
w	wall
∞	ambient

daily temperature swing from day to night. Similarly, daytime ventilation (mechanical and natural) was determined to be applicable and energy efficient for all buildings. However, in regions that lack wind speed such as high density cities where the building's structure blocks the wind field, replenishing indoor air for occupant thermal comfort can be achieved only by mechanical ventilation [11–13]. Zhou et al. [14] discussed the effect of coupling the thermal mass and natural ventilation on the passive building design. They tested different wall configurations and found that heavy walls with external insulation provide the lowest amplitude of indoor air temperature among different external low mass walls.

In terms of natural material, wood, sisal, jute, bamboo, coconut, asbestos, rockwool and hemp are examples that can be used. Along those lines, an innovative building material that has shown to yield multiple socio-economic benefits is Hempcrete. Hempcrete is a mix of cement mortar with fibers of industrial hemp, a sister plant of cannabis. The benefits of using hemp have been reported by a study conducted by Awwad et al. [15]. The study shows that Hempcrete: (i) improves physical characteristics and structural performance of concrete; (ii) reduces raw materials and energy resources and (iii) provides a material with better thermal property and therefore increases energy efficiency. With such benefits, and being a carbon neutral material, the use of hemp in concrete reduces the embodied energy of concrete and other cementitious materials which are widely used and in large quantities in building construction.

This paper further investigates options to lower operational energy without negatively affecting embodied the energy of typical apartments in urban and rural settings by conducting research that considers both the building materials and a mechanical ventilation system for comfort and air quality. The paper focuses, through a case study in Lebanon on the use of local and regional materials such as strawboard for insulation and hemp in concrete that contribute to the decrease in the building embodied and operational energy. In addition, the paper proposes a space

model for controlling the amount of ventilation air needed for conditioning the building's indoor environment. The paper does not consider natural ventilation as there are many uncontrollable variables (blockage of urban wind by high rise building, uncontrolled outside air velocity, security issues) which could affect its reliability as an effective air conditioning option. Mechanical ventilation and ceiling fans are used to adjust the indoor air temperature and speed whenever needed to achieve thermal comfort. Any fluctuations in outside temperature or solar load can cause the internal air temperature to fluctuate in a similar way, though delayed and dampened depending on the thermo-physical properties (thermal capacitance, resistance and density) of the building wall construction materials as well as its layering arrangement. The effectiveness of mechanical ventilation in achieving thermal comfort for a given building construction material is determined through the reliability of this system in offering thermal comfort without having the need to resort to mechanical cooling during summer and winter operations.

2. Mathematical formulation

To meet the objective of this paper, a mechanical ventilation controller integrated with a numerical multi-zonal space and comfort model is developed (Fig. 1). For given building materials and a set of indoor and outdoor conditions, the ventilation controller modulates the amount of ventilation air needed to moderate the indoor air temperature and minimize discomfort hours. Different building materials are assessed for both their effect on indoor comfort and fan consumption. The numerical space model is validated against other commercial simulation software that simulates indoor air temperature for Lebanon conditions.

2.1. Space model

The space analyzed in the case study is divided into two zones: living and bedroom. The transient one-dimensional heat conduction equation for a multilayered wall consisting of N parallel layers is given by the following equation:

$$\rho_{i,j} c_{i,j} \frac{\partial T_{i,j}(t, x)}{\partial t} = k_{i,j} \frac{\partial^2 T_{i,j}(t, x)}{\partial x^2} \quad (1)$$

where i represents building element (wall, ceiling, or floor), j represents the j th layer within the element i , t and x are the time and spatial coordinates respectively, T_{ij} is the temperature, whereas k , ρ , and c are the thermal conductivity, density, and thermal capacity respectively.

The boundary conditions for the outdoor and indoor surfaces of the wall are

$$\alpha \cdot I(t) + h_{c\infty} [T_{\infty}(t) - T_i(0, t)] + h_{r\infty} [T_{sky}(t) - T_i(0, t)] = -k \frac{\partial T_{i,j}(0, t)}{\partial x} \quad (2)$$

$$h_{ca} [T_i(L, t) - T_a(t)] + \sum_{j=1}^6 h_{r_{i-j}} [T_i(L, t) - T_j(t)] = -k \frac{\partial T_i(L, t)}{\partial x} \quad (3)$$

where the external radiative coefficient, $h_{r\infty}$, is equal to $\varepsilon \sigma (T_{sky} + T_i(0, t))(T_{sky}^2 + T_i^2(0, t))$ and the internal radiative coefficient, $h_{r_{i-j}}$, is equal to $\varepsilon \sigma F_{i-j} (T_i(L, t) + T_j(t))(T_i^2(L, t) + T_j^2(t))$. The coefficients h_{ca} and h_r are the convective and radiative heat transfer coefficients for the outdoor and indoor wall surfaces respectively, α is the wall surface absorptivity, and I is the total solar radiation on the wall side. The temperatures T_{∞} , $T(0, t)$, $T_a(t)$, $T(L, t)$ and T_{sky} are the ambient air and outside wall surface temperature, room air, inner wall surface temperature, and sky temperature.

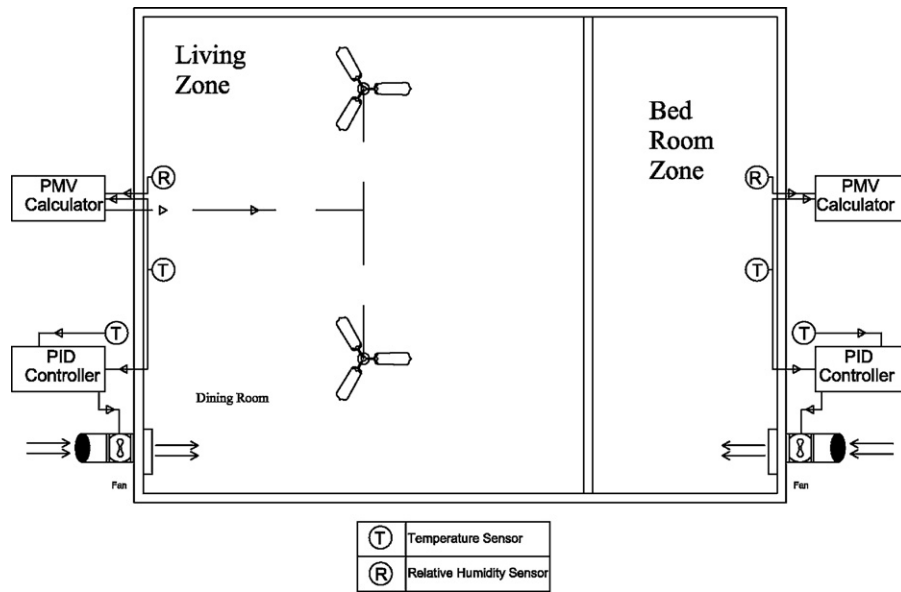


Fig. 1. Schematic of the ventilation system coupled with the PID controller.

Neglecting infiltration, the internal lumped air node energy balance is given by

$$\rho_a V_a c_{p,a} \frac{\partial T_a(t)}{\partial t} = \sum_{i=1}^6 h_{c,a} \cdot A_i (T_i - T_a) + \dot{m} c_{p,a} (T_\infty - T_a) + \sum q_{\text{int}} \quad (4)$$

where ρ_a , V_a , and c_a are density, volume and specific heat capacity of the room air respectively, A_i and T_i are the surface area and the temperature of the room element i , \dot{m} and T_∞ are the mass flow rate and the temperature of the air supplied by the ventilation system. q_{int} is the internal heat load.

Eq. (5) represents simplified dynamic moisture for the space, as follows:

$$\rho_a V_a \frac{d w_a}{d t} = G - \dot{m} (w_a - w_\infty) \quad (5)$$

where G is the rate of moisture generation inside the space due to latent loads, w_a and w_∞ are the room air and supply air humidity ratios.

2.2. Thermal comfort model

Different thermal comfort model are discussed in several studies [16–20]. The new adaptive comfort model for ASHRAE standard 55 address thermal comfort in naturally ventilated building. In this standard the temperature range that satisfies thermal comfort of people is higher than the other conservative approaches based on the predicted mean vote (PMV) method [18,19]. However, this standard is limited to building with reachable and operable windows that is controlled by human. For this reason, in this research the predicted mean vote (PMV) model [18] is used to assess the indoor thermal comfort. The PMV represents the thermal sensation of people on a scale from -3 (cold) to $+3$ (hot). The model is simple, widely used by researchers and its input requirements are direct and can be categorized as environmental (temperature, relative humidity, air velocity,) and personal (clothing insulation and metabolic rate). Thermal comfort inside the space is calculated on an hourly basis, based on the room hourly average temperature, average relative humidity and air velocity for the precedent hour. Comfort inside the space is assumed to occur when the PMV inside the space is between -1 and $+1$.

2.3. Controller equation

A PID controller is used to modulate the ventilation air flow rate based on room temperature and indoor fresh air requirement [21]. Every 5 min, the controller updates the ventilation air flow rate to keep the indoor air temperature at its summer and winter set points and to provide thermal comfort for longer periods, if possible, as indoor air temperature deviates from its set point.

The indoor air temperature is controlled using the following equation:

$$\begin{aligned} \dot{m}_{(t)} = & \dot{m}_{(t-1)} + \left(K_c \left(1 + \frac{\Delta t}{T_I} + \frac{TD}{\Delta t} \right) \times (T_{\text{room}} - T_{\text{set point}}) \right. \\ & - \left(1 + 2 \frac{TD}{\Delta t} \right) \times (T_{\text{room}} - T_{\text{set point}})_{(t-1)} + \frac{TD}{\Delta t} \\ & \left. \times (T_{\text{room}} - T_{\text{set point}})_{(t-1)} \right) \end{aligned} \quad (6)$$

where Δt is the time step, K_c , T_I and TD are the proportional, integrative and derivative gains parameters. These parameters are tuned to track the setpoint temperatures by determining the amount of air flow rate needed to minimize the difference between the indoor air temperature and the setpoint temperature.

3. Numerical simulation methodology

As mentioned earlier, the space and comfort models are integrated with the ventilation controller model into one transient model. The model is capable of determining the amount of ventilation air that can possibly provide indoor thermal comfort for longer periods and prevent large deviations of indoor air temperature from its set point during summer and winter operations. The transient model is simulated to obtain the indoor zone thermal comfort when subjected to variable external and internal loads. This requires the following information: the space dimensions, characteristics of the construction materials, outdoor weather conditions, external and internal loads and the ventilation controller operation conditions (e.g. activation and deactivation modes). Eq. (1) is solved numerically using the finite difference method with a fully implicit scheme where each wall layer is decomposed into a number of volumes, each having one node. The program is developed using MATLAB[®]

(2010). The total number of nodes used in each wall layer is 120 nodes.

Starting from arbitrary initial conditions, and using a time step of 2.5 min, the inner surface temperatures of the space walls are computed along with the inner air temperature. This time step represents a compromise between accuracy and simulation runtime. Simulations are performed for typical weather conditions of each month to obtain the effectiveness of the mechanical ventilation system in providing thermal comfort throughout the entire day. At the end of the 24 h operational period of each month, the initial conditions are recalculated and used as input in the cyclic simulations until steady periodic convergence is achieved. The criterion for convergence is reached when the maximum percentage error for air temperature between the simulation values at time t and $t + 24$ h is less than $10^{-4}\%$.

3.1. Control strategy

The strategy that is used to condition the indoor environment relies on controlling the amount of air brought to the space during summer and winter operation. The outdoor air is allowed to vary between a minimum and an upper limit. The minimum limit is determined by the fresh air requirement of 7.5 l/s/person (recommended by ASHRAE [16]), whereas the upper limit is set to 25 ACH which is close to what has been reported by Geros et al. [11] and Shaviv et al. [12] as the maximum effective rate of air change for an hour. The controller varies the amount of fresh air between the two limits to maintain an indoor temperature close to the winter and summer set points whenever the outdoor conditions allow. Otherwise, the controller prevents large deviations between indoor and outdoor temperatures. The control strategy depends on different parameters such as: the type of zone (living or bedroom), the time (day or night) and the season (winter or summer).

For the living zone, the control is active during the day (after 8 in the morning) and remains active till hour 23. During non-occupancy period (23–8), in the summer season, night purging with constant air flow is applied into the space; the supplied outdoor air flow takes advantage of the low temperature profile during night time throughout the summer season and helps purging the internal loads accumulated in the space during the day, while in winter the minimal requirement are applied to the space. Different values for night purging have been used in literatures [6,10,12]. During summer season, an air change per hour of 5 ACH, is close to what has been used in the Middle East region [12] and close to what has been reported by Kolokotroni and Aronis [6] and Blondeau et al. [7], and is therefore used in this paper. As for the bedroom zone, the control is active during the occupancy time (23 till 10).

The season is a main parameter in the controller strategy; thus, the following strategy is used during the activation time period: for the winter period (November through March), the controller is set to activate whenever the indoor air temperature is lower than the outdoor ambient temperature, provided that it is lower than the winter set point temperature of 22 °C, ($T_{\text{room}} < T_{\text{amb}}$ and $T_{\text{room}} < T_{\text{set point}}$). On the other hand, during the summer period (April through October), if the indoor air temperature is lower than the outdoor ambient temperature ($T_{\text{room}} < T_{\text{amb}}$), the amount of ventilation air entering the space is set to the minimum amount of fresh air requirement recommended by ASHRAE [16]. The controller is activated whenever the indoor air temperature is higher than the outdoor ambient temperature ($T_{\text{room}} > T_{\text{amb}}$) provided that the indoor air temperature is higher than the set point temperature of 26 °C ($T_{\text{room}} > T_{\text{set point}}$). If thermal comfort is not attained, a ceiling fan is turned on concurrently to increase the indoor air velocity to 1.5 m/s.

In order to minimize the fluctuation resulting from consecutive activation and deactivation of the controller, the air temperature

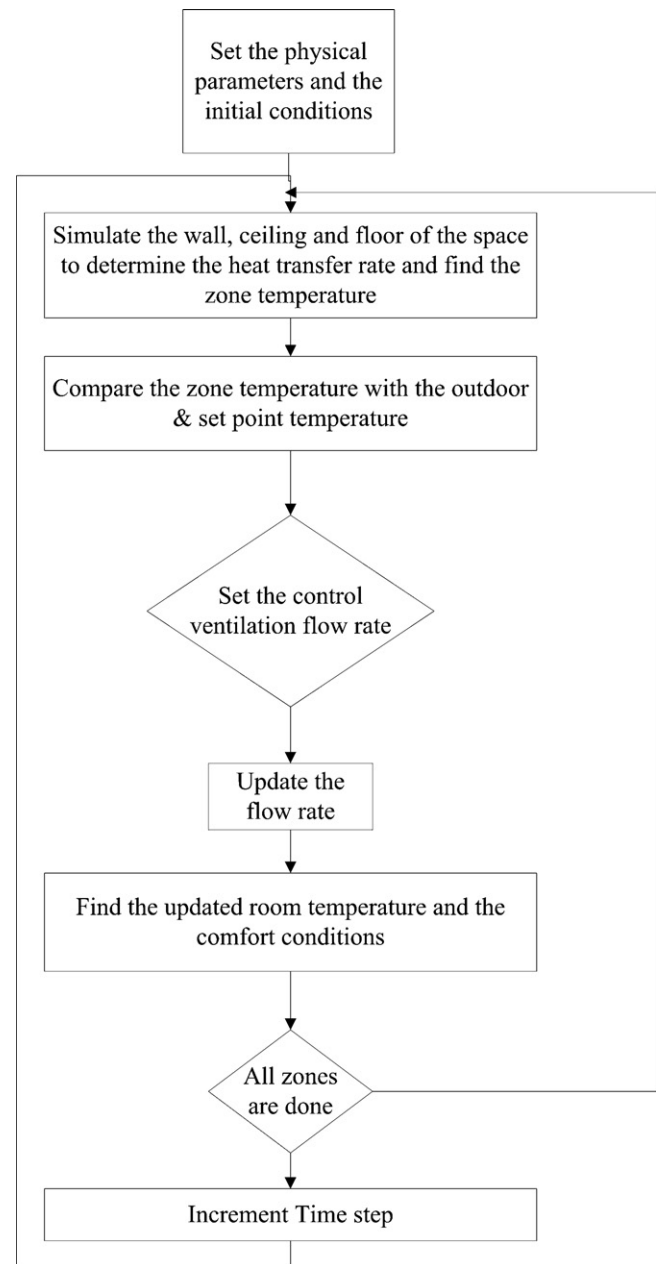


Fig. 2. Numerical model flow chart (urban setting).

and the mass flow rate at time (t) are compared to those at time $(t - 1)$. If the difference is less than 5% for one of the two parameters, then the same mass flow rate at time $(t - 1)$ is used at time (t) and the indoor air temperature is simulated for this amount of air flow. Fig. 2 presents the flow chart of the proposed numerical model.

4. Validation of the numerical model

To ensure that the results of the numerical model are realistic and represent the real conditions of a typical residential apartment in Beirut, Lebanon, the numerical model should be validated against calibrated software such as TRNSYS which is known for its flexibility in modeling mechanical ventilation [22]. This requires making sure that the results of the numerical model are accurate and also simulate the actual conditions of residential apartments in Beirut. Therefore, TRNSYS was first calibrated and then used to validate the numerical space model [22]. To calibrate TRNSYS, a

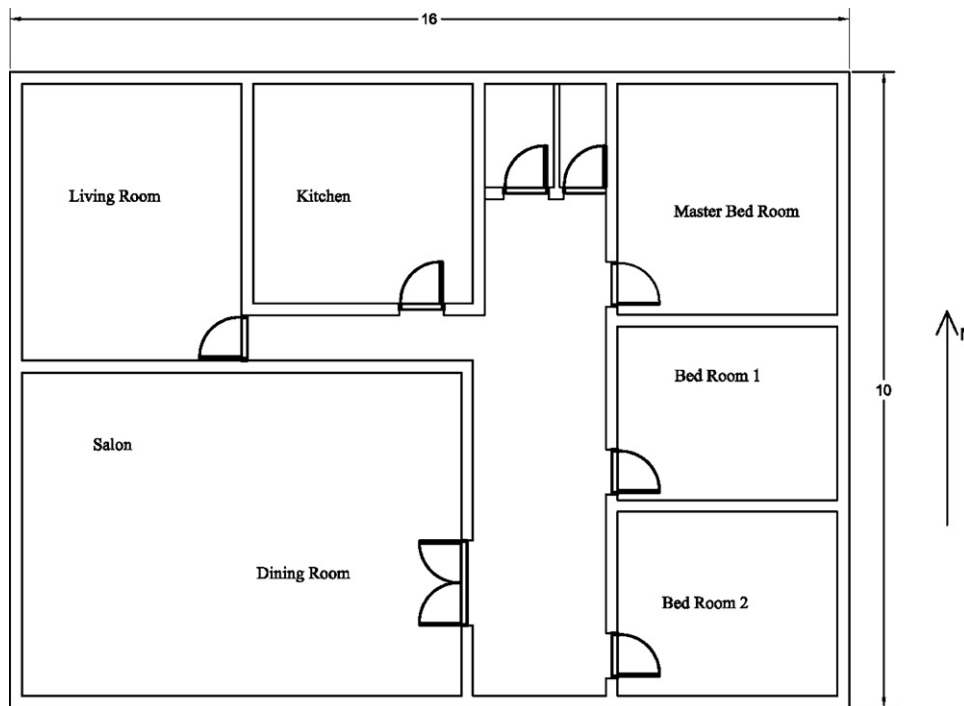


Fig. 3. Typical apartment plan in Beirut.

typical apartment in Beirut (base case) is simulated, and the results are compared against published data on energy consumption for a typical residential apartment in Lebanon city by Hourri and Orfali [23] and Karaki et al. [24]. This is done by entering the data of a typical residential house in Beirut, including building structural data, operational and occupancy schedule, internal loads and outdoor climatic conditions.

Once calibrated, results from TRNSYS can serve as a benchmark to validate the results obtained from the numerical model, in a two-step process. The first step is to run the simulation software, resulting in 181 values (180 values during occupancy period (15 h) in addition to a constant flow rate during non-occupancy (8 h)). These values are then input from the numerical model into TRNSYS. The second step is to compare the simulated indoor air temperature provided by the numerical model to that provided by TRNSYS. The following sections elaborate on the validation effort.

4.1. Base case description

As mentioned earlier, a typical apartment in Beirut is considered as a base case in this paper. The apartment is assumed to have a $16\text{ m} \times 10\text{ m}$ square layout and a height of 3 m as shown in Fig. 3. It is divided into two zones: living zone (dining and living rooms) and bedroom zone (three bedrooms). The living zone has an area of 100 m^2 while the bedroom zone has an area of 60 m^2 . The zones have a common partition wall and 3 external walls each. The external walls are made of 15 cm concrete masonry blocks with 1.5 cm lay mortar cement plaster on the internal and external sides of the wall, while the internal partition wall is only 10 cm thick. The external walls have an overall heat transfer coefficient of $2.36\text{ W/m}^2\text{ K}$ and a heat capacity of 1200 J/kg and the internal partition has an overall heat transfer coefficient of $3.63\text{ W/m}^2\text{ K}$, which is typical for urban residential apartments in Lebanon [25,26]. The living zone

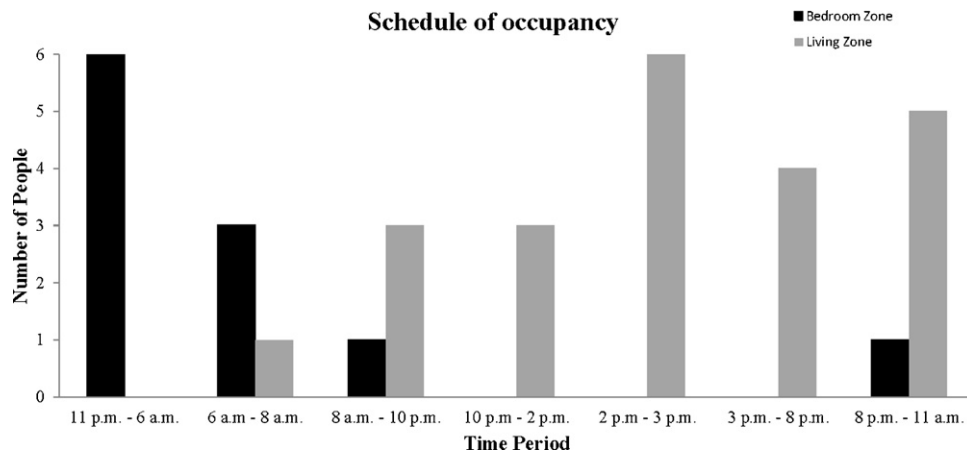


Fig. 4. Schedule of the people load inside the apartment.

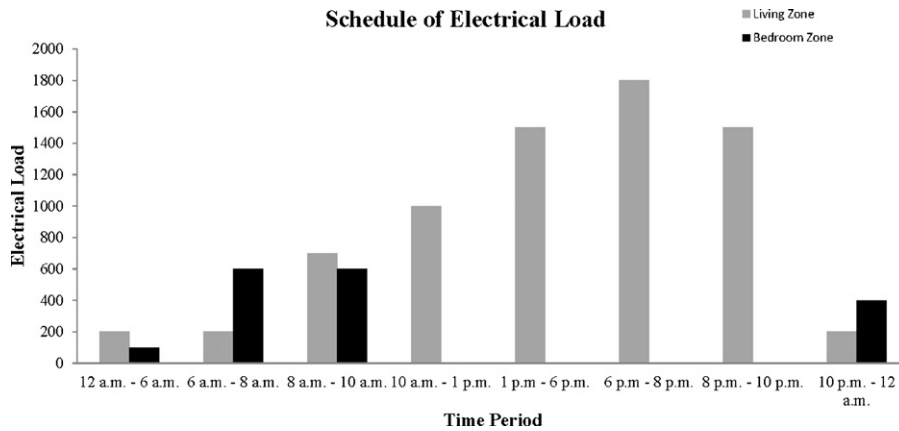


Fig. 5. Schedule of the electrical load inside the apartment.

has three external walls oriented to the North, South and West direction with an area of 30 m², while the bedroom has two external walls of 18 m² area oriented the North and South, and a 30 m² wall oriented to the East.

The internal load component is based on the occupancy schedule of a typical Lebanese family consisting of 6 persons [25]. Fig. 4 shows the hourly variation in occupancy between the two zones. The electrical loads are 10 W/m² of sensible load for lighting fixture sand 800 W for appliances (refrigerator, TV and PC). Fig. 5 presents the schedule of the electrical load in both the living and bedroom zones. The schedule is assumed to apply for the whole year.

4.2. Base case calibration

A simulation of the base case using TRNSYS [22] showed a peak cooling load of 14.05 kW occurring at hour 16 on July 28th, with an annual cooling requirement of 132.8 kWh/m², and a heating peak load of 5.49 kW occurring at hour 6 in the morning on February 12th with an annual heating requirement equal to 27.8 kWh/m². The weather data (outdoor air temperature, solar radiation and the relative humidity) is obtained from the records of the Mechanical Engineering Department at the American university of Beirut.

The simulations are made on an intermittent basis. During summer season, the cooling mode is activated and the heating mode is switched off; however, the system is scheduled to turn off when the temperature inside the space is lower than the set point temperature (26 °C). On the other hand, during the winter season, the

heating mode is activated and the cooling mode is switched off when the temperature is higher than the set point temperature (22 °C). The total base case heating and cooling needs during the whole year are equal to 160.60 kWh/m²/year of thermal energy. Using a typical energy performance of a split unit HVAC system at an average COP of 3.0, the total annual electric energy consumption of the cooling and heating system in the base case is equal to 53.53 kWh/m².

The total electrical energy consumption of the base case is compared against published data on the electrical energy consumption of a residential house with similar dimensions in Beirut. Karaki et al. [24] reported that HVAC systems consume 50% of the total electrical energy consumption in residential houses in Lebanon at an approximate consumption rate of 48 kWh/m² [23], which is 10% different than the yearly energy consumption calculated by TRNSYS [22]. Fig. 6 shows the monthly energy consumption calculated by TRNSYS versus the results documented by Ghaddar and Bsatt [27]. A maximum deviation of 10% is found between the published and the TRNSYS simulated monthly data.

4.3. Comparison against TRNSYS

In order to make sure that the proposed numerical model is yielding accurate results for the zone conditions, the model is run for the living zone on August 21st and November 21st. The simulation results of the ventilation airflow rates of the numerical model are used as input in the simulation of TRNSYS to compare the

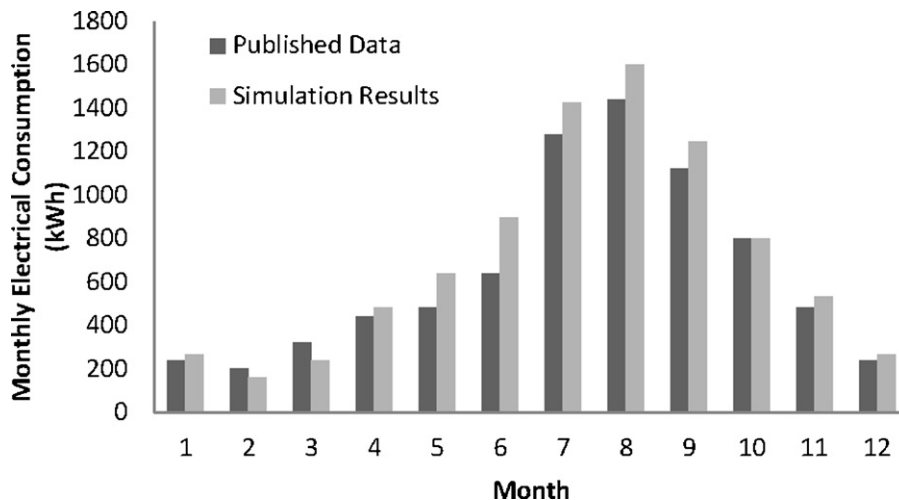


Fig. 6. Reported and simulated monthly electrical consumption of HVAC system.

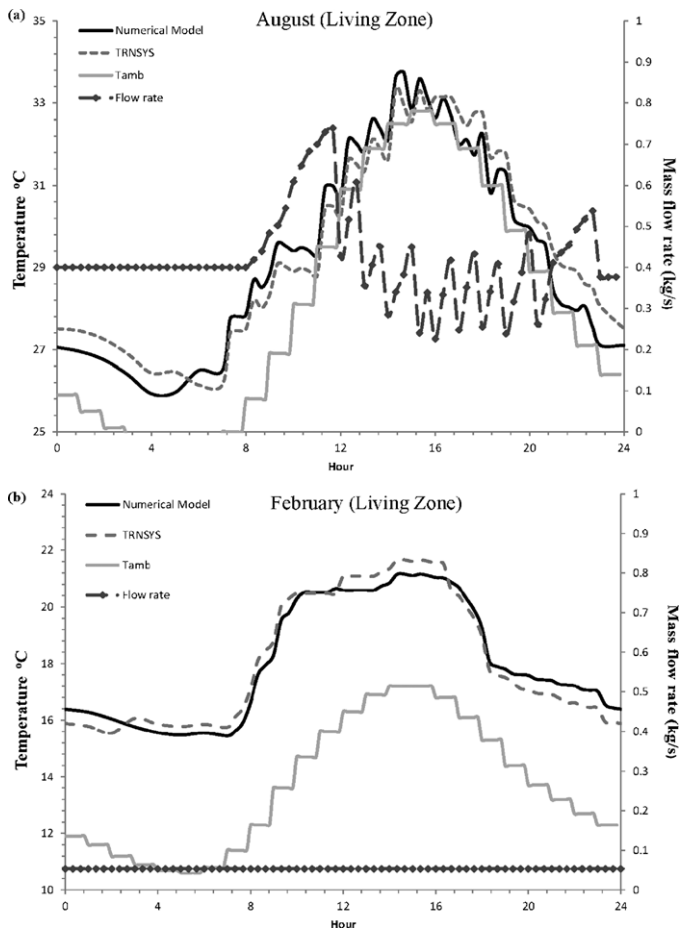


Fig. 7. Comparison between the numerical model and TRNSYS [22] software of the temperature and air mass flow rate in the living zone for the months of (a) August, and (b) February.

resulting indoor air temperature of the numerical model and TRNSYS. Fig. 7(a) and (b) shows that the space temperature, predicted by the two models, is comparable with a difference of $\pm 4\%$.

5. Simulation results and discussion

As mentioned earlier, the base case apartment shown in Fig. 3, which is divided into two zones (living and bedroom zones), is considered as a test case for the proposed integrated space, thermal comfort, and ventilation control model. Simulations are carried out for a representative day, i.e. the 21st of each month of the year, for the city of Beirut, Lebanon. In order to obtain accurate results independent of the initial conditions, simulations are performed for 3 consecutive days, and the data for the third day are adopted in the analysis described in the following section.

5.1. Alternative cases

To attain the objective of identifying building materials and configurations which may optimize a building energy requirements, two configurations, in addition to the base case, were examined for each of the living and bedroom zones resulting in seventy-two simulations (six simulations for each month). Several wall configurations of different building materials and wall thickness are considered for the two zones, living and bedroom. In both zones, Hempcrete is used as an alternative for the conventional concrete mix used for the masonry blocks. Hempcrete has lower thermal conductivity and higher thermal capacitance compared with the

conventional hollow concrete block, and a lower embodied energy [15].

The investigated configurations focus on selecting building materials that result in high insulation and capacitance in the living room zone, and low insulation and capacitance in the bedroom zone. Two wall configurations were considered for the living zone. Case 1 consists of 3 cm of straw ($C_p = 2000 \text{ J/kg K}$) sandwiched between 2 cm \times 6 cm of Hempcrete ($C_p = 1430 \text{ J/kg K}$). Case 2 (massive case) consists of 5 cm of straw sandwiched between 2 cm \times 10 cm of Hempcrete. Two additional configurations (Cases 3 and 4) were considered for the bedroom wall. Case 3 consists of 10 cm of Hempcrete, and Case 4 is made of 10 cm of Hempcrete and 5 cm of straw board placed on the internal side. The thermal properties of straw were obtained from "the green building bible" [28] and the thermal properties of hemp were obtained from Elfordy et al. [29]. Table 1 summarizes the various investigated configurations.

6. Results

Figs. 7–12 present the indoor air temperature for the different wall configurations, for the months of (a) February, (b) April and (c) August, representative months for the winter, spring and summer seasons. The fan power consumption is calculated based on the affinity law for prime movers. The fan power is proportional to the cube of the flow rate ratio taken with respect to a reference. During the month of February, the mechanical ventilation controller is set to the deactivation mode for both zones (living and bedroom) since the indoor air temperature is lower than the set winter temperature and higher than the outdoor air temperature throughout the whole simulation day resulting in a fan consumption of 0.96 kWh for all the cases. For the living zone indoor temperature shown in Fig. 8(a) and (c), the base case wall configuration (Fig. 8(a)) characterized by lower thermal capacitance showed an indoor air temperature profile that respond to the outdoor temperature variations much more than the wall configurations for Case 1 (Fig. 8(b)) and Case 2 (massive wall, Fig. 8(c)). The thermal characteristics of the wall base case resulted in having a total of 7 discomfort hours as compared to 6 discomfort hours for Case 1 and 3 discomfort hours for Case 2. The temperature inside the living zone of Case 2, shown in Fig. 8(c), tends to be constant during the non-occupancy period, and increases slightly during the occupied time. As for the bedroom zone, simulations during the month of February indicate that the wall with lowest insulation (Case 3) corresponds to the lowest air temperature as shown in Fig. 9(b). This is due to a higher amount of heat loss between the indoor and the outdoor spaces. The wall with the highest insulation ($U = 0.98 \text{ W/m}^2 \text{ K}$, $C_{p, \text{straw}} = 2000 \text{ J/kg K}$, Case 4) seems to have better conditions in the winter season since it has a higher indoor air temperature as can be seen in Fig. 9(c) and lower number of discomfort hours. Case 4 has five discomfort hours occurring during the hour period 5 till 10 compared to six and seven discomfort hours for the base case and Case 3 respectively.

In the month of April (Fig. 10), night purging is applied in the living zone, and since the temperature inside the space during the occupied period is less than the set temperature, the controller is set to the deactivation mode resulting in a fan consumption of 3.32 kWh in the three cases. Both the base case and Case 1 showed an indoor living zone temperature higher than the outdoor air temperature with a general lower indoor air temperature profile for the base case (Fig. 10(a) and (b)). As for the massive wall configuration (Case 2), the high capacitance of the wall results in having an indoor air temperature that is lower than the outdoor during the hour period of 8–15 and higher than the outdoor for the rest of the occupied period (see Fig. 10(c)). In the bedroom zone (Fig. 11), the control was also set to the deactivation mode during the occupancy time, resulting in a fan consumption of 0.96 kWh. The wall

Table 1
Different examined scenarios of wall configuration of living and bedroom zones.

Zone	Scenario	Wall configuration	U value (W/m ² K)
Both zone	Base case	15 cm hollow concrete	2.36
Living zone	Case 1	3 cm of straw sandwiched between 2 cm × 6 cm of Hempcrete	1.37
Bedroom zone	Case 2 (massive case)	5 cm of straw sandwiched between 2 cm × 10 cm of Hempcrete	0.7
	Case 3	10 cm of Hempcrete	3.1
	Case 4	10 cm of Hempcrete + 5 cm of straw	0.986

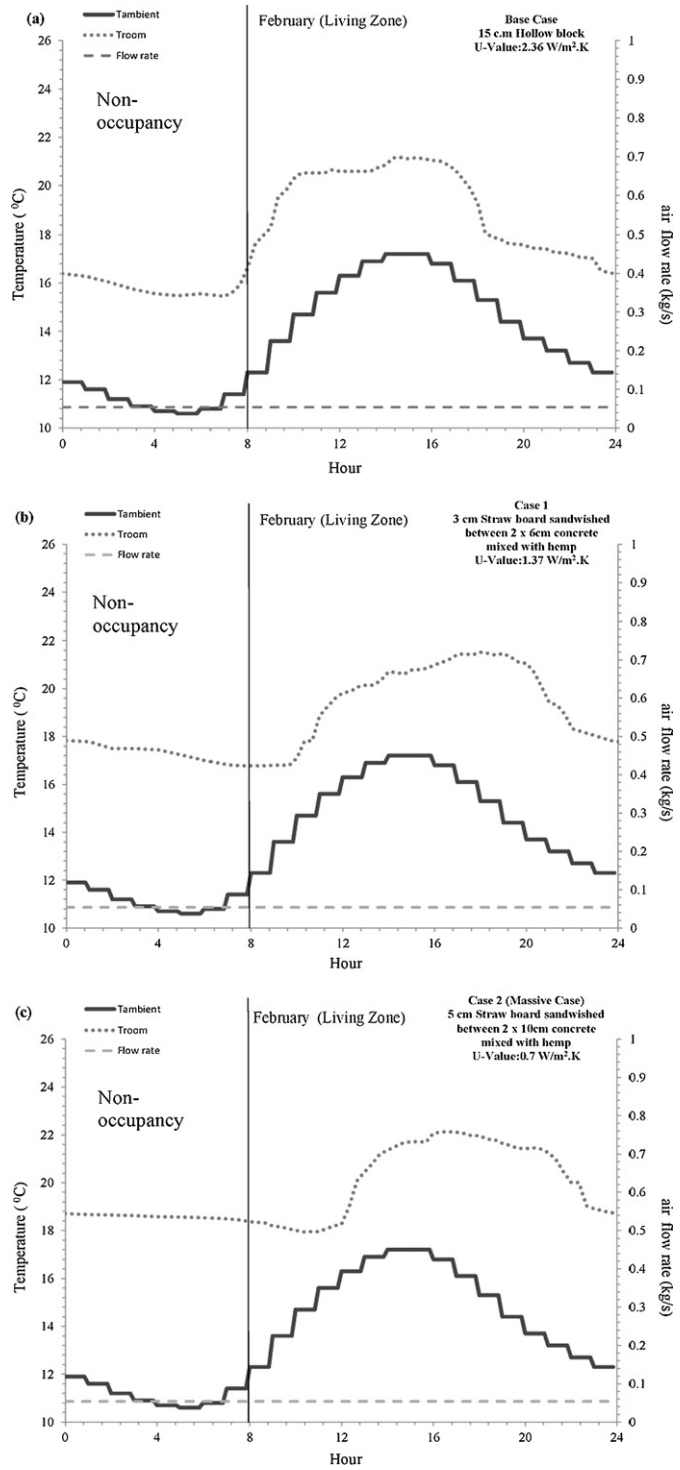


Fig. 8. Temperature and mass flow rate in the living zone during February for (a) base case, (b) Case 1, and (c) Case 2 (massive case).

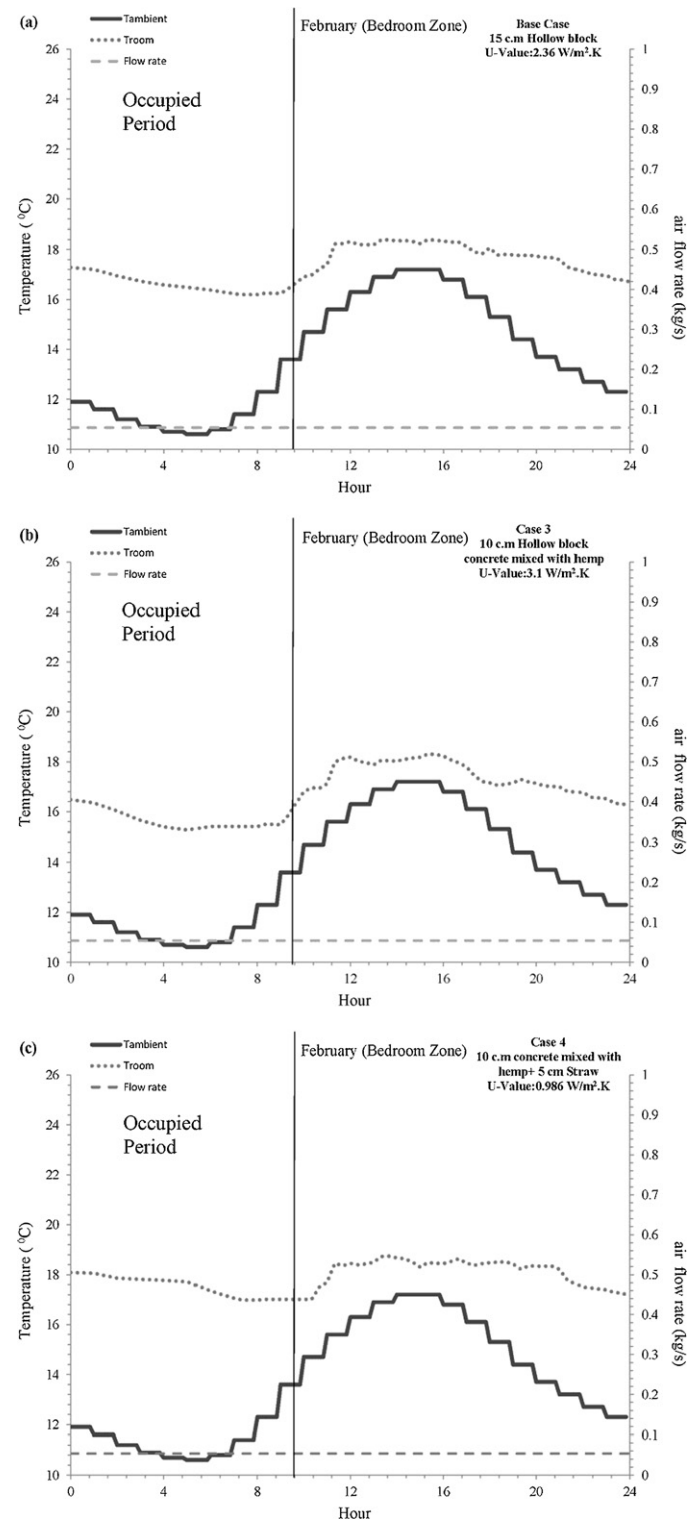


Fig. 9. Temperature and mass flow rate inside the bedroom zone during February for (a) base case, (b) Case 3, and (c) Case 4.

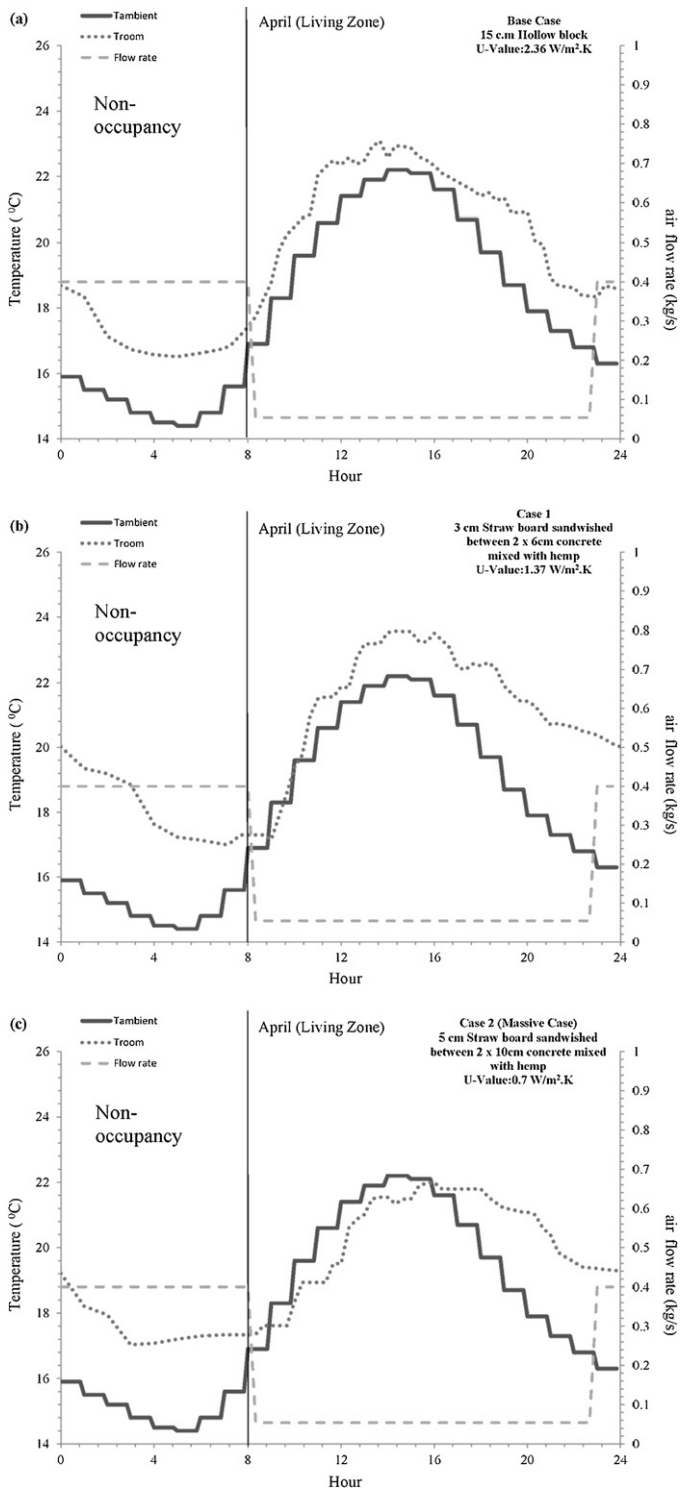


Fig. 10. Temperature and mass flow rate in the living zone during April for (a) base case, (b) Case 1, and (c) Case 2 (massive case).

case of the highest insulation (Case 4) has the highest air temperature profile, and due to its highest thermal capacitance, the temperature inside the space takes more time to increase during the non-occupied period (see Fig. 11(c)). Case 3, which is characterized by the lowest insulation, had the lowest temperature profile (see Fig. 11(b)). No discomfort hours were recorded in the different cases for both the living and bedroom zones.

In August, the controller modulated the outdoor ventilation air flow to prevent the indoor air temperature from increasing beyond

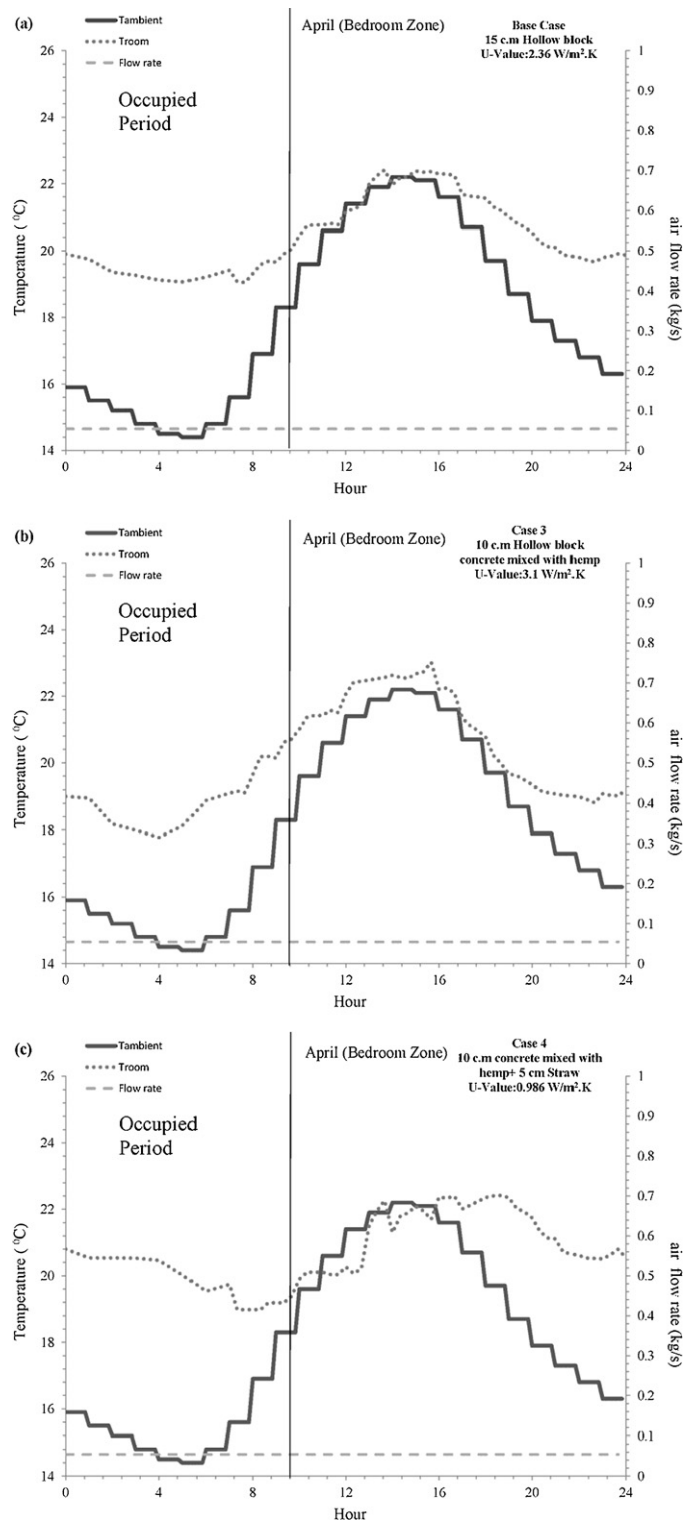


Fig. 11. Temperature and mass flow rate inside the bedroom zone during April for (a) base case, (b) Case 3, and (c) Case 4.

the outdoor air temperature for both wall configuration, Cases 1 and 2. Fig. 12(b) and (c) shows a lower indoor air temperature than in the base case shown in Fig. 12(a). However, since comfort cannot be achieved at the indoor air temperature, the ceiling fan was turned on to improve comfort conditions inside the space for the period hour extending from 12 to 20 and to limit the discomfort hours to seven during the hour period of 13–20 in comparison to 12 and 11 discomfort hours for the base case and Case 1 respectively.

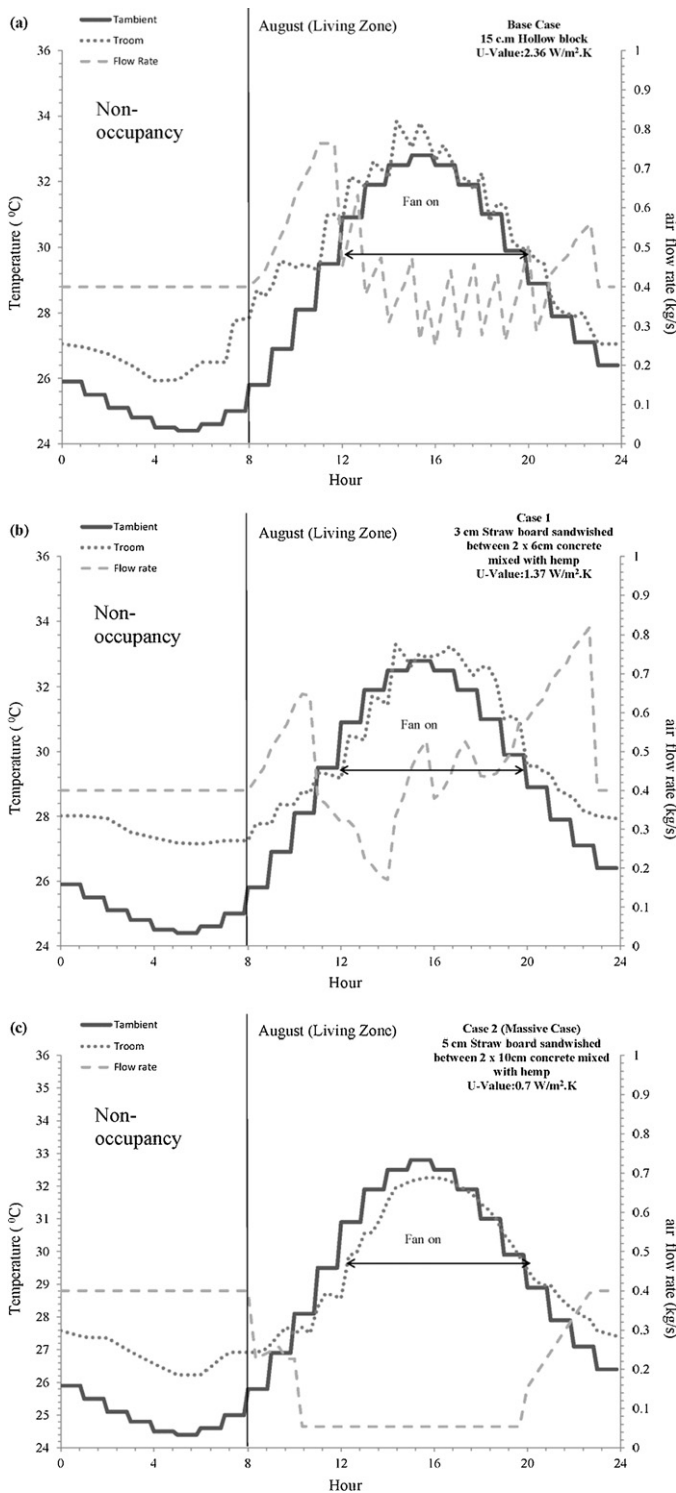


Fig. 12. Temperature and mass flow rate in the living zone during August for (a) base case, (b) Case 1, and (c) Case 2 (massive case).

In the bedroom zone, Case 3 (Fig. 12(b)), which is characterized by the highest heat transfer coefficient, had the lowest indoor air temperature at the early hours of the occupied period as compared to the bedroom air temperature of the base case (Fig. 12(a)) and Case 4 (Fig. 12(c)). Two hours of discomfort Thermal comfort was attained inside the space during occupancy with zero discomfort hours for Case 3 against 2 h of discomfort for the two other bedroom wall cases (base case and Case 4), moreover due to the lower wall insulation of Case 3, less ventilation air is needed to moderate

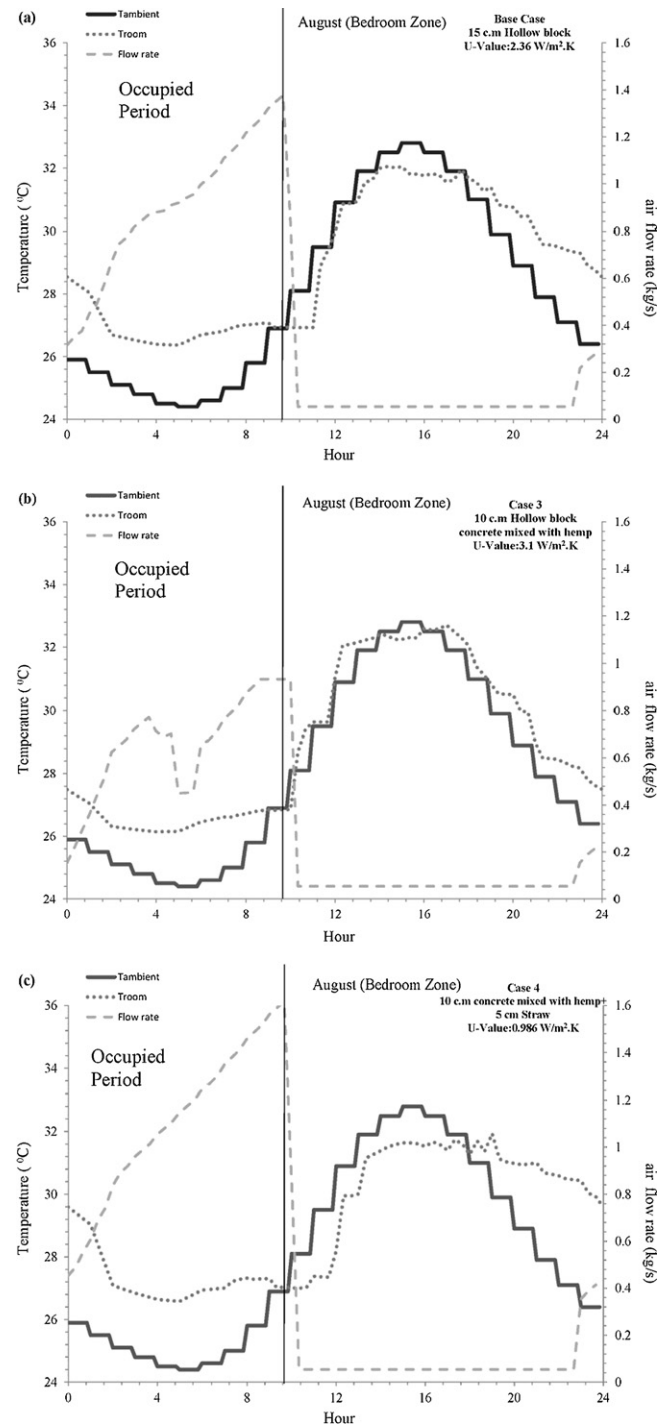


Fig. 13. Temperature and mass flow rate inside the bedroom zone during August for (a) base case, (b) Case 3, and (c) Case 4.

the indoor zone temperature (5.70 kWh) as compared to the base case (7.65 kWh) and (9.39 kWh) for wall Case 4 (Fig. 13).

The numerical model was run for the six simulations (three for each of the living and bedroom zones) for the representative day of each month of the year. The results were multiplied by the number of days in each month to determine the monthly number of discomfort hours in each zone as shown in Fig. 14(a) and (b), and the monthly fan consumption as shown in Fig. 15(a) and (b) for the different scenarios.

As shown in Figs. 14 and 15, Case 2 (massive wall in the living zone) has the lowest operational energy and lowest number

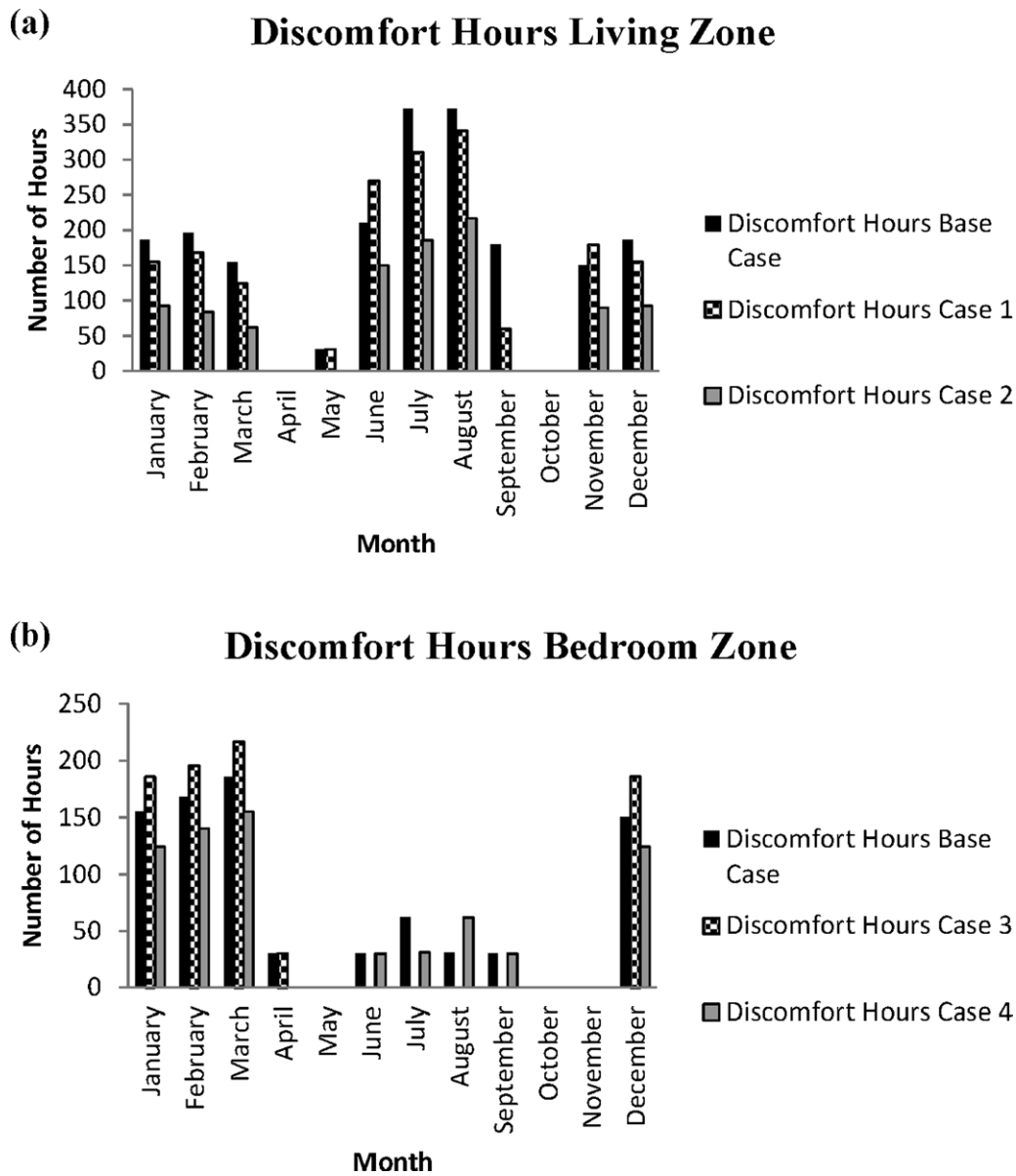


Fig. 14. Number of discomfort hours for the different cases for (a) living zone and (b) bedroom zone.

of discomfort hours during the whole year as compared to the other living zone wall cases. As for the bedroom zone, the base case and Case 3 have approximately equal number of yearly discomfort hours (842 discomfort hour in the base case, and 815 in Case 3); however, even though the high thermal wall insulation, Case 4, has the lowest number of discomfort hours (696 discomfort hour) but it turns to be an in-effective solution for the bedroom since it has a 25.9% increase in the fan energy consumption. On the other hand, bedroom wall Case 3, compared to the base case, can decrease the fan energy consumption by 18.6% and decrease the discomfort hours by 3.2%. However, the discomfort hours mainly occur in the winter during hours when occupants are expected to be sleeping.

From Table 2, it is clear that the use of a mechanical ventilation system for the base case can save around 40.5% of operational energy consumption of the conventional air conditioning system while having 2880 discomfort hours, 32.8% of discomfort hours during the year. The energy consumption can be reduced by 26.9% and the discomfort hours can be reduced by 37.8% when using wall

Table 2

Mechanical ventilation electrical consumption and number of yearly discomfort hours for the different cases.

Configuration wall case	Yearly electrical consumption (kWh/m ²)	Number of yearly discomfort hours
Base case (mechanical heating and cooling)	53.53	Not applicable
Base case (mechanical ventilation) (living + bedroom)	31.80	2880
Living zone base case	14.32	2038
Living zone Case 1	15.57	1794
Living zone Case 2	9.02	975
Bedroom zone base case	17.48	842
Bedroom zone Case 3	14.22	815
Bedroom zone Case 4	22.01	696

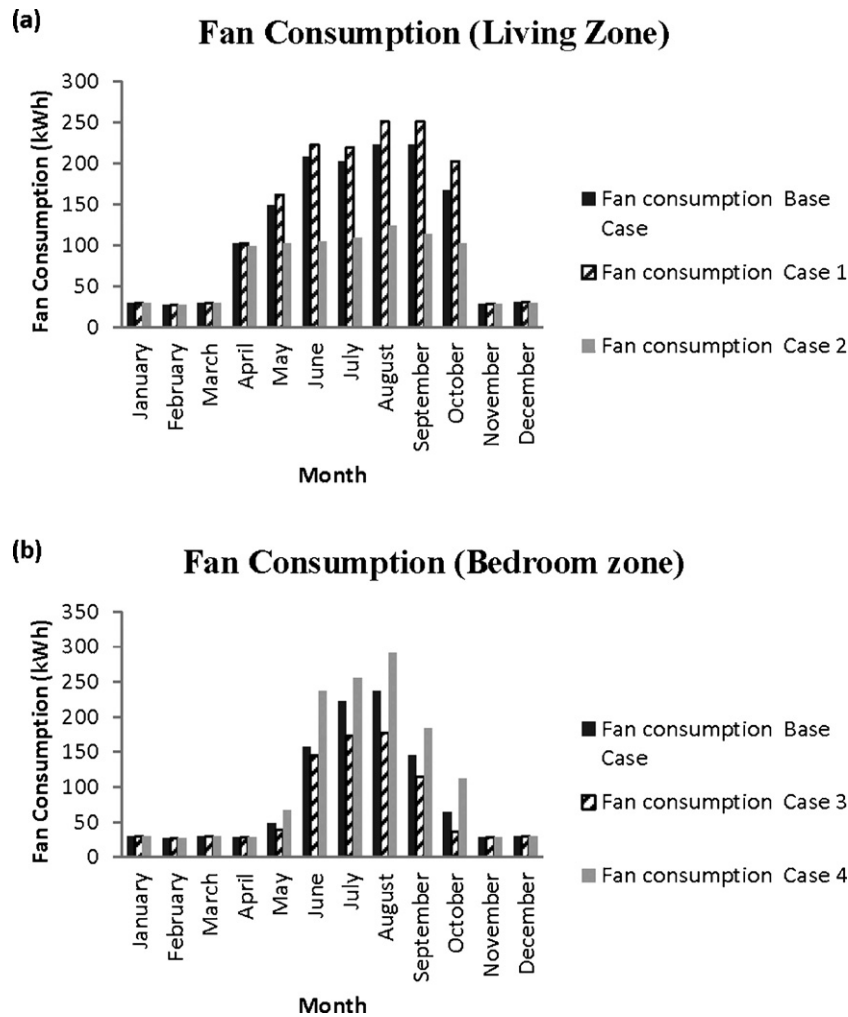


Fig. 15. Fan consumption for the different cases for (a) living zone and (b) bedroom zone.

configuration of Case 2 in the living zone and wall configuration of Case 3 in the bedroom zone.

7. Conclusion

This paper integrates space and comfort and ventilation controller models into one model. Through simulation, the integrated model determines the amount of ventilation air that can possibly provide indoor thermal comfort for longer periods. This allows for accurately measuring the energy performance of buildings and assessing the operational energy of various building envelop designs.

In order to validate the simulation results, a typical house in Beirut, Lebanon, is modeled in TRNSYS [22]. This required calibrating TRNSYS against published data, and then comparing the results against the proposed numerical model. The analysis confirmed that the building design parameters affect the thermal comfort inside the space and fan consumption of the mechanical ventilation system. The simulation results revealed that a combination of a massive wall made of a 5 cm layer of straw sandwiched between 2 cm × 10 cm of Hempcrete in the living zone, and in addition to 10 cm of Hempcrete in the bedroom zone, can reduce the operational cost of the house by 26.9% and the discomfort hours by 37.8% compared to the base case.

Acknowledgment

The financial support of the Munib Masri Institute for Energy and Natural Resources at the American University of Beirut is highly acknowledged.

References

- [1] UNEP-SBCI, Buildings and Climate Change: Status, Challenge and Opportunities, UNEP Publication, Paris, France, 2007.
- [2] P. Kesselring, C.J. Winter, World energy scenarios: a two-kilowatt society, plausible future or illusion? in: Proceedings of the Energietage 94, Villigen, Switzerland November 10–12, 1994.
- [3] A. Pfeiffer, M. Koschenz, A. Wokaum, Energy and building technology for the 2000 W society potential of residential buildings in Switzerland Energy and Building 37 (2005) 1158–1174.
- [4] T.F. Schulz, S. Kypreos, L. Barreto, A. Wokaum, Intermediate steps towards the 2000 W society in Switzerland: an energy-economic scenario analysis, Energy Policy 36 (2008) 1303–1317.
- [5] Le. Tran, C. Maalouf, T.H. Mai, E. Wurtz, F. Collet, Transient hydrothermal behavior of a hemp concrete building envelope, Energy and Building 42 (2010) 1797–1806.
- [6] M. Kolokotroni, A. Aronis, Cooling-energy reduction in air-conditioned offices by using night ventilation, Applied Energy 63 (4) (1999) 241–253.
- [7] P. Blondeau, M. Spérandio, F. Allard, Night ventilation for building cooling in summer, Solar Energy 61 (5) (1997) 327–335.
- [8] H. Breesch, Passive cooling in a low-energy office building, Solar Energy 79 (2005) 682–696.

- [9] G. Carrilho da Graca, Q. Chen, L.R. Glicksman, L.K. Norford, Simulation of wind driven ventilative cooling systems for an apartment building in Beijing and Shanghai, *Energy and Buildings* 34 (2002) 1–11.
- [10] U. Eicker, Ling strategies, summer comfort and energy performance of a rehabilitated passive standard office building, *Applied Energy* 87 (6) (2010) 2031–2039.
- [11] V. Geros, M. Santamouris, A. Tsangrasoulis, G. Gurracino, Experimental evaluation of night ventilation phenomena, *Energy and Buildings* 29 (1999) 141–154.
- [12] E. Shaviv, A. Yezioro, I.G. Capeluto, Thermal mass and night ventilation as passive cooling design strategy, *Renewable Energy* 24 (3–4) (2001) 445–452.
- [13] B. Givoni, Indoor temperature reduction by passive cooling systems, *Solar Energy* 85 (8) (2011) 1692–1726.
- [14] J. Zhou, G. Zhang, Y. Lin, Y. Li, Coupling of thermal mass and natural ventilation in buildings, *Energy and Building* 40 (2008) 979–986.
- [15] E. Awwad, B. Hamad, M. Mabsout, H. Khatib, Sustainable construction material using hemp fibers – preliminary study, in: Second International Conference on Sustainable Construction Materials, June 28–June 3, 2010.
- [16] ASHRAE, ASHRAE Standard 55, Thermal Environmental Conditions for Human Occupancy, ASHRAE, Atlanta, 1992.
- [17] ASHRAE, Climate, Comfort, and Natural Ventilation: A New Adaptive Comfort Standard for ASHRAE Standard 55, University of California, Berkeley, 2001.
- [18] P.O. Fanger, Thermal Comfort, Danish Technical Press, Copenhagen, 1970.
- [19] E. Kruger, Thermal monitoring and indoor temperature predictions in a passive solar building in an arid environment, *Energy and Building* 43 (2008) 1792–1804.
- [20] H. Zhang, E. Arens, C. Huizenga, T. Han, Thermal sensation and comfort models for non-uniform and transient environments: part I: local sensation of individual body parts, *Building and Environments* 45 (2) (2010) 380–388.
- [21] R. Dorf, R. Bishop, Modern Control Systems, 11th ed., Pearson International Edition Pearson Education, 2008.
- [22] TRNSYS, Transient System Simulation Tool Software. Thermal Energy System Specialists, LLC. Madison Wisconsin. <http://www.tess-inc.com/>, (accessed 25.06.12).
- [23] A. Hourri, S. Orfali, Residential energy consumption patterns: the case of Lebanon, *International Journal of Energy Research* (2005) 755–766.
- [24] S. Karaki, F. Chaaban, R. Chedid, T. Mezher, A. Harb, A. Abdulla, A. Hamzeh, A. Yahia, Electric energy access in Jordan, Lebanon and Syria, in: Proceedings of International Conference on Energy Research and Development (ICERD-3), Kuwait, 2005.
- [25] Republic of Lebanon Ministry of Public Works and Transport. Energy Analysis and Economic Feasibility. UNDP/GEF, MPWT/DGU, 2005, p. 63.
- [26] United Nation Development Program, Lebanon Page, <http://www.undp.org.lb/programme/pro-poor/poverty/povertyinlebanon/conditions97.cfm>, (accessed 17.06.12).
- [27] N. Ghaddar, A. Bsat, Energy conservation of residential buildings in Beirut, *International Journal of Energy Research* 22 (1998) 523–546.
- [28] Hall Keith (Ed.), The Green Building Bible, vols. 1 and 2, 3rd ed., The Green Building Press, 2006.
- [29] S. Elfordy, F. Lucas, F. Tancret, Mechanical and thermal properties of lime and hemp concrete (“hempcrete”) manufactured by a projection process, *Construction and Building Materials* 22 (2008) 2116–2123.